Electronic Supplementary Material (ESI) for RSC Advances.

Ultrafast synthesis of near-zero-cost S-doped $Ni(OH)_2$ on C_3N_5 at ambient condition with enhanced photocatalytic activity

Lixiao Han#, Cong Peng#, Jinming Huang, Shengyao Wang, Xiaohu Zhang, Hao Chen, Yi Yang*

College of Science, Huazhong Agricultural University, Wuhan 430070, PR China

yiyang@mail.hzau.edu.cn

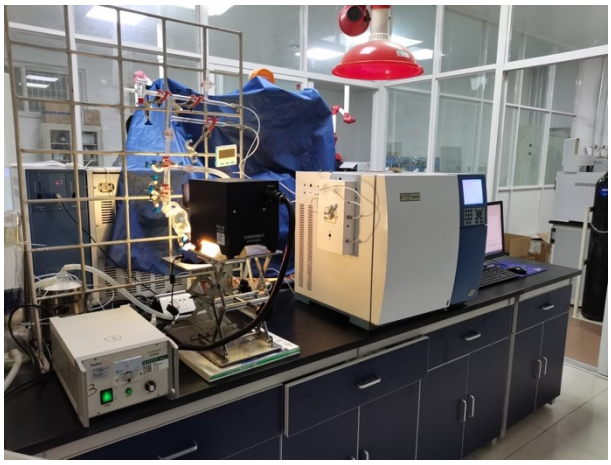

Fig. S1. The photograph of photocatalytic H_2 system.

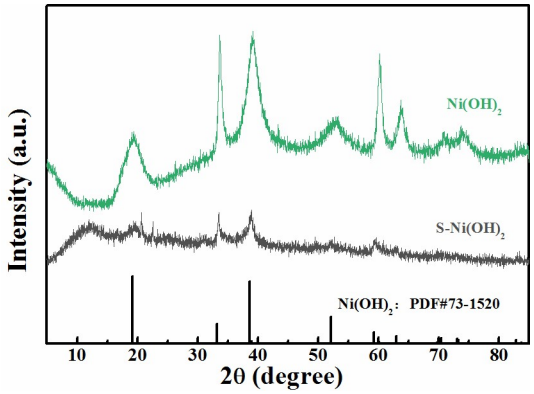

Fig. S2. XRD patterns of S-$Ni(OH)_2$ and $Ni(OH)_2$.

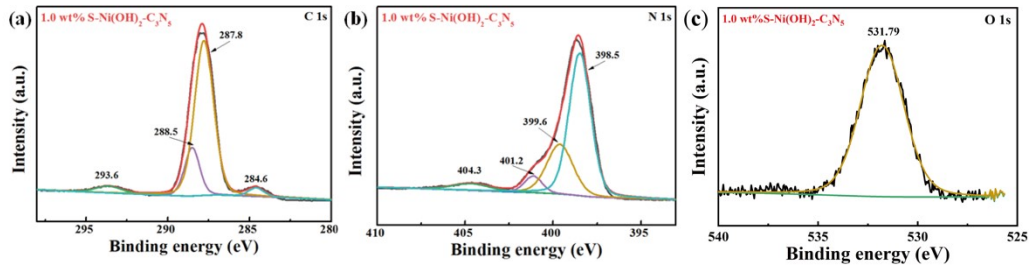

Fig. S3. High-resolution XPS spectra of C 1s (a), N 1s (b), and O 1s (c) of 1.0 wt% S-$Ni(OH)_2$-C_3N_5.

Table S1. The element content of C, N, S, (determined by elemental analysis) and Ni (determined by ICP-MS) of the prepared S-$Ni(OH)_2$-C_3N_5 materials.

Samples	N (wt%)	C (wt%)	S (wt%)	Ni (wt%)
0.5 wt% S-$Ni(OH)_2$-C_3N_5	59.38	32.91	0.341	0.3
1.0 wt% S-$Ni(OH)_2$-C_3N_5	57.64	31.42	0.555	0.98
2.0 wt% S-$Ni(OH)_2$-C_3N_5	56.5	31.26	1.509	1.6

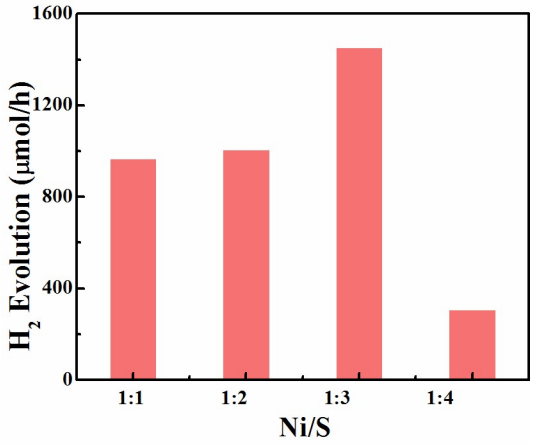

Fig. S4. Influence of mol ratio of Ni^{2+}/Na_2S on the H_2 production activity of 1.0 wt% S-$Ni(OH)_2$-$Ni(OH)_2$.

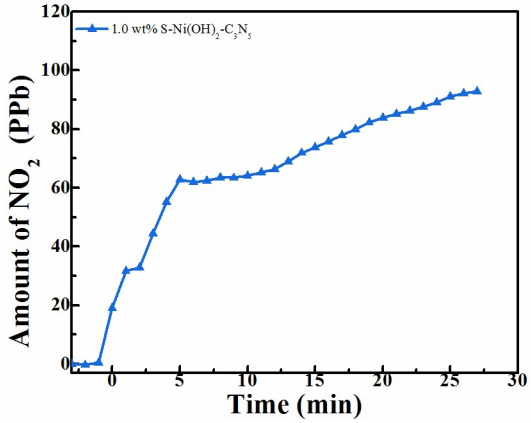

Fig. S5. Change tendency of NO_2 during NO oxidation procedure over 1.0 wt% S-$Ni(OH)_2$-C_3N_5.

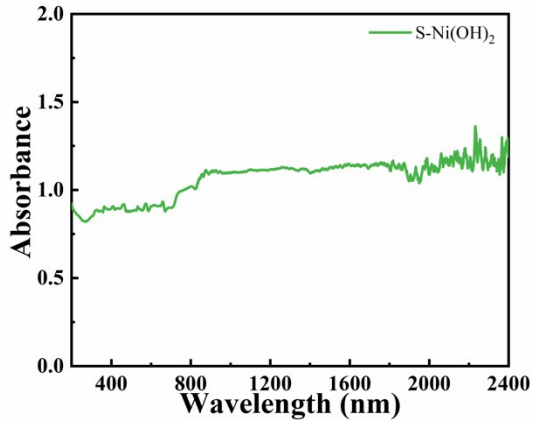

Fig. S6. The solid-state UV-Vis-NIR diffuse reflectance spectra (DRS) of S-Ni(OH)$_2$.

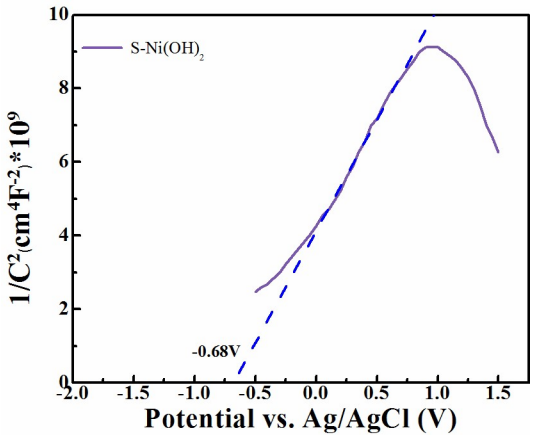

Fig. S7. The Mott‐Schottky plots of S-Ni(OH)$_2$.

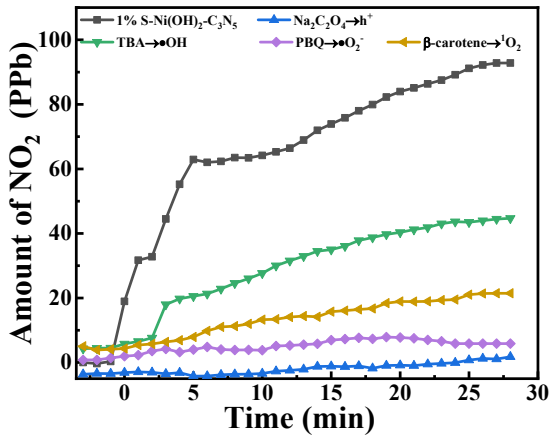

Fig. S8. The NO_2 concentration during the photocatalytic NO removal with scavengers on 1.0 wt% S-Ni(OH)$_2$-C_3N_5.

Table S2. The residual ratio of NO_2 by using different scavengers on 1.0 wt% S-$Ni(OH)_2$-C_3N_5.

*Scavenger	No scavenger	$Na_2C_2O_4$ (h^+)	TBA (•OH)	PBQ ($•O_2^-$)	β-carotene ($^1O_2$)
**Residual ration of NO_2	26.4%	2.0%	**40.7%**	20.0%	**35.0%**

* $Na_2C_2O_4$ for h^+, TBA for •OH, PBQ for $•O_2^-$ and β-carotene for $^1O_2$

**Residual ration of NO_2=$C_{NO2}/\Delta C_{NO}$